Three-Dimensional Distribution of Air Pollutants in the Los Angeles Basin

RUDOLF B. HUSAR AND DAVID E. PATTERSON

Air Pollution Research Laboratory, Department of Mechanical Engineering, Washington University, St. Louis, Mo. 63130

DONALD L. BLUMENTHAL, WARREN H. WHITE[1] AND THEODORE B. SMITH

Meteorology Research, Inc., Altadena, Calif. 91001

(Manuscript received 28 May 1976, in revised form 18 August 1977)

ABSTRACT

Data from a three-dimensional pollutant mapping program, conducted in the Los Angeles basin, were analyzed to obtain "grand average" vertical profiles sampled on 24 summer days in 1973. Morning and afternoon profiles at four locations show an erosion of the nighttime radiation inversion, increased temperatures, more intense mixing in the inland areas, and a semi-permanent subsidence inversion at higher levels. High values of primary pollutant parameters (NO_x and condensation nuclei) are seen in the western part of the basin at Hawthorne. Secondary pollutant parameters (O_3 and light scattering coefficient) were dominating at the inland receptor site, Riverside. Ozone concentrations in the morning were consistently higher aloft. The deficit near the surface is attributed to ozone scavenging by primary emissions.

1. Introduction

The experience of observing the smog layer from a descending airplane is probably the most convincing demonstration of the three-dimensional nature of the Los Angeles smog. In the summer months of 1972 and 1973, the Three Dimensional Pollutant Gradient Study was conducted to map the vertical and horizontal pollutant structure, and to study the transport and transformation processes in the Los Angeles basin. Two aircraft made soundings, in the form of vertical spirals, from the top of the polluted layer to the surface at 17 locations with an average of about 40 spirals for each location. Three meteorological parameters, temperature, relative humidity and turbulence (energy dissipation rate), as well as five pollutants, O_3, NO_x, CO, light scattering coefficient and condensational nuclei, were monitored continuously along with the necessary coding and position parameters. A list of the instruments used and their characteristics is given in Table 1.

The three-dimensional pollutant mapping program improved substantially our understanding of the pollutant transport and transformation processes in the Los Angeles basin. The data indicate complex and varying patterns of these processes from one time or location to another. Detailed inspection of the data revealed, however, that certain phenomena are so characteristic for a given location or time period that they survive extensive averaging.

In this paper, we present and discuss the "grand average" vertical profiles measured over the airports of Hawthorne, El Monte, Ontario and Riverside. Their respective locations in the basin are shown in Fig. 1. All 165 soundings, conducted on 24 days in 1973 at these locations, were used to calculate the mean and standard deviation of all measured parameters for each location, time period (A.M. or P.M. PDT) and hundred-foot altitude increment.

The average profiles presented in this section are calculated from a sample population which was biased toward photochemical smog conditions as mapping was intentionally restricted to days with above average smog potential. Although they cannot be taken as representative on an overall basis, the mean profiles should be fairly typical of conditions during smoggy summer and early fall days since they are drawn from data on 24 days of this type. It is hoped that the findings presented here will have utility in the assessment of average transport and transformation processes and in providing information for the testing of three-dimensional diffusion-transformation models.

2. Meteorological parameters

a. Temperature

A primary factor in the production of high pollutant concentrations in Los Angeles air is the fre-

[1] Present affiliation: 1180 North Chester, Pasadena, Calif. 91104.

TABLE 1. Aircraft instrumentation.

Instrument	Ranges available	Time response (90%, for usual ranges)
1. MRI Integrating Nephelometer	10*, 40, 100×10^{-4} m^{-1}	1 s
2. Environment One Condensation	1, 3, 10, 30, 100*, 300* 10K×10^{3} CN cm^{-3}	5 s
3. REM 612 Ozone Monitor (chemiluminescent)	50*, 200 pphm	5 s
4. REM 642 NO–NO$_x$ Monitor (chemiluminescent)	0.5*, 2*, 10 ppm	5 s
5. Andros 7000 CO Monitor (dual isotope fluorescence)	20, 50*, 100, 200 ppm	5 s
6. MRI Airborne Instrument Package		
Temperature	−5 to +45°C	5 s
Humidity	0 to 100%	30 s
Turbulence	0 to 10 cm$^{\frac{3}{2}}$ sec^{-1}	3 s (to 60%)
Altitude	0 to 10 000 ft	1 s
Indicated air speed	50 to 150 mph	$\leqslant$ 1 s
7. Metrodata M/8 VOR Analog Converter (uses aircraft radio)		1 s
8. Metrodata 620 Data Logger (20 channels)		48 channels per second

* Range normally used.

quent occurrence of temperature inversions which restrict the vertical dispersion of pollutants. This phenomenon is evident in Fig. 2, which shows the mean morning and afternoon temperature profiles at Hawthorne, El Monte, Ontario and Riverside. In the mean morning profiles at all four locations, the temperature of the air at 3000 ft MSL is higher than the temperature of the air near the surface, with a negative lapse rate from 3000 ft down almost to the surface. As the day progresses, the surfaces of inland areas of the basin are heated by the sun, warming the air near the ground and eroding the inversion from below (Edinger, 1973). By afternoon, the mean profiles for all three inland locations show a well-defined layer at the surface in which the lapse rate is adiabatic.

The effect of surface heating is seen from another perspective in Fig. 3a, which displays the mean afternoon temperature profiles for the four sampling locations. At Hawthorne the afternoon profile is little changed from the morning profile due to the stabilizing influence of the nearby ocean. As air moves inland with the usual afternoon flow, however, temperatures near the surface increase, eroding the inversion. The

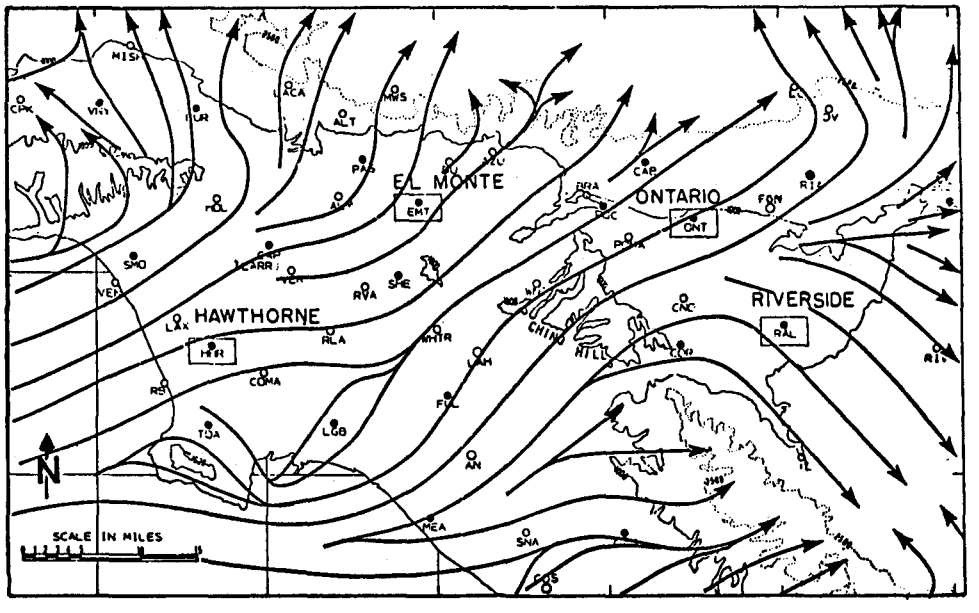

FIG. 1. Map of the Los Angeles air basin indicating the locations where the "grand average" profiles were calculated. Streamlines show most frequent afternoon surface winds during July (after Blumenthal *et al.*, 1974).

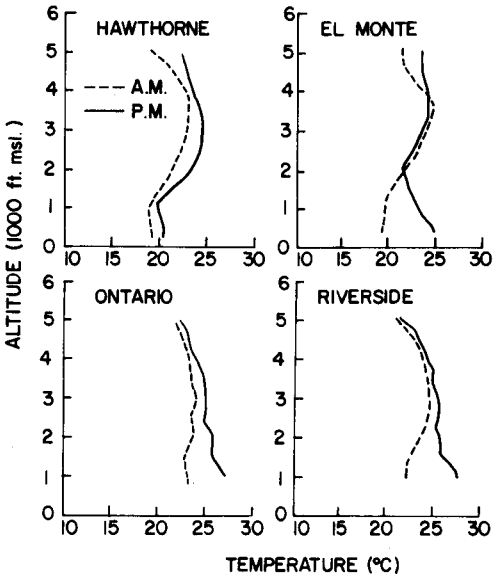

FIG. 2. Mean morning and afternoon temperature profiles.

unstable layer at the surface deepens until, at Ontario and Riverside, it may "break through" the inversion.

b. Turbulence

The mean profiles of small-scale turbulence intensity (Fig. 4), as indicated by the energy dissipation coefficient $\epsilon^{\frac{2}{3}}$ (MacCready, 1964), are compatible with the mean thermal structure. In the morning, when air is stable, turbulence is confined to a shallow layer at the surface where it is generated by mechanical effects and surface heating. In the afternoon, turbulence extends about 1000 ft above the morning mixing layer. In all profiles, the intensity of the turbulence decreases with height until it reaches a "background" value of about $\epsilon=0.5$ cm$^{\frac{2}{3}}$ s^{-1}, reflecting the decay of small-scale turbulence with increasing height.

c. Relative humidity

Mean afternoon profiles of relative humidity are shown in Fig. 3b. Mean morning and afternoon relative humidities are generally in the range 30–50%, except in the mixing layers at Hawthorne and Riverside.

3. Reactive gases

a. Nitrogen oxides

The first two oxides of nitrogen are important participants in the photochemistry of the Los Angeles atmosphere. Photodissociation of NO_2($NO_2+h\nu\rightarrow NO+O$) starts the chain of reactions leading to the buildup of ozone. Oxidation of NO($NO+O_3\rightarrow NO_2+O_2$) limits the rate of this buildup in its early stages.

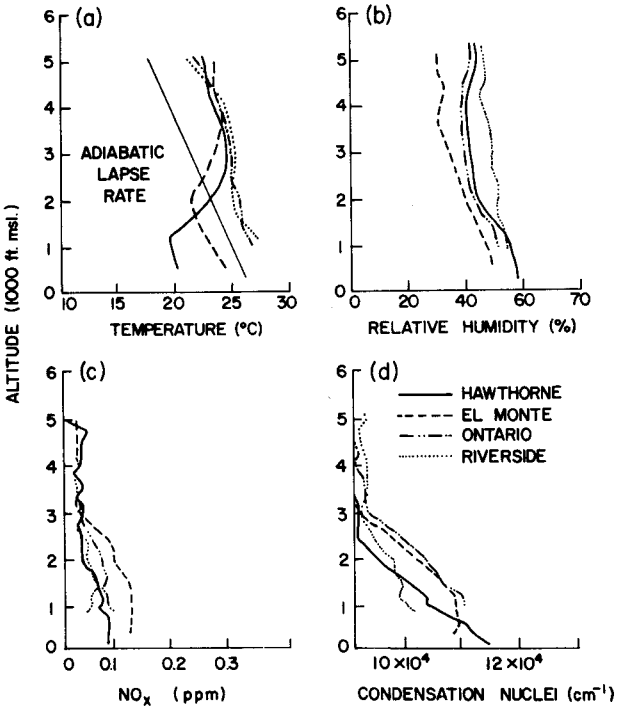

FIG. 3. Mean afternoon profiles of temperature, humidity, NO_x and condensation nuclei at the four sampling sites.

Although these two reactions affect the relative concentrations of NO and NO_2 in the air, they leave invariant their sum, the concentration of NO_x. NO_x is formed almost exclusively by combustion sources such as motor vehicles and power plants and is lost

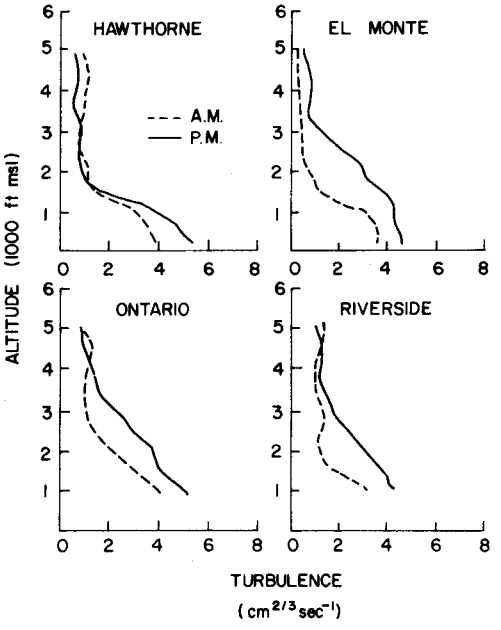

FIG. 4. Mean morning and afternoon turbulence profiles.

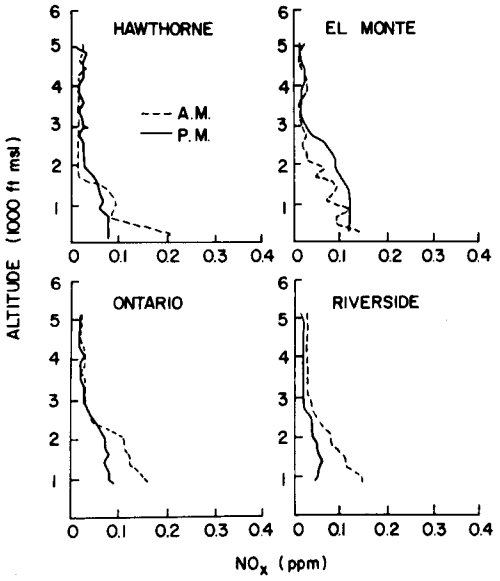

FIG. 5. Mean morning and afternoon NO_x profiles.

through reactions with surfaces and by the formation of nitrates.

Mean profiles of NO_x concentration are shown in Figs. 5 and 3c. Substantial concentration gradients appear near the surface in the morning profiles due to the generally poor mixing prevailing at this time. By afternoon, concentrations become fairly uniform through the unstable mixing layer. In both morning and afternoon profiles, mean concentrations drop to about 0.03 ppm above the mixing layer.

The smallest values for mean NO_x concentrations and the integral of these concentrations with respect to height are seen in the afternoon profile for Riverside. The latter half of a typical afternoon trajectory to Riverside passes over a predominantly rural area, where emissions of NO_x are apparently not sufficient to balance losses by aerosol formation and dry deposition. Peroxyacetyl nitrate (PAN) concentrations at Riverside can reach 0.05 ppm on smoggy days (Lundgren, 1970). Particulate nitrate concentrations >100 μg m^{-3}, equivalent to over 0.04 ppm of NO_x, were measured there during the 1973 Aerosol Characterization Study (Hidy *et al.*, 1974). The measured high concentrations of PAN and particulate nitrates indicate that a substantial fraction of the NO_x emitted in the western portion of the air basin is converted to nitrates. It is also likely that a further, at present, unknown fraction of NO_x is lost to vegetation and ground (Hill, 1971) enroute to Riverside.

b. Ozone

Unlike NO_x, ozone is not emitted directly, but is formed in the atmosphere through the sequence of reactions initiated by the photodissociation of NO_2. In reacts very rapidly with NO, the principal constituent of NO_x emissions, so that fresh emissions of NO_x tend to lower, rather than raise, O_3 concentrations. These characteristics are clearly demonstrated in the mean profiles of O_3 (Fig. 6).

Note that ozone concentrations do not drop to background levels ($\sim$0.04 ppm) above the mixing layer. At Hawthorne, for example, the mean temperature, turbulence and NO_x profiles all indicate a mixing layer strongly confined below 2000 ft MSL, yet the mean O_3 concentration at 3000 ft MSL is 0.1 ppm, greater than the federal standard. Mechanisms by which polluted air occurs above the mixing layer are discussed elsewhere (Blumenthal *et al.*, 1974). What is important in the present context is that the O_3 at 3000 ft over Hawthorne is part of a polluted air mass which has aged above the mixing layer. In the absence of scavenging by fresh NO_x emissions, which are confined within the mixing layer, reactions have proceeded almost to completion, producing relatively large ozone concentrations from small concentrations of NO_x and hydrocarbons.

A second feature of the mean profiles which is unique to O_3 is the occurrence of deficits near the surface. The most striking example of this is the morning profile at Hawthorne, where mean O_3 concentrations near the surface are under 0.02 ppm, less than the 0.04 ppm background levels observed in clear air. In fact, all four morning profiles as well as the afternoon profile at Hawthorne, show ozone concentrations which are lower within the mixing layer than they are immediately above it. These O_3 deficits are due principally to scavenging by fresh emissions of NO_x which are trapped within the shallow, well-defined mixing layers exhibited in these profiles.

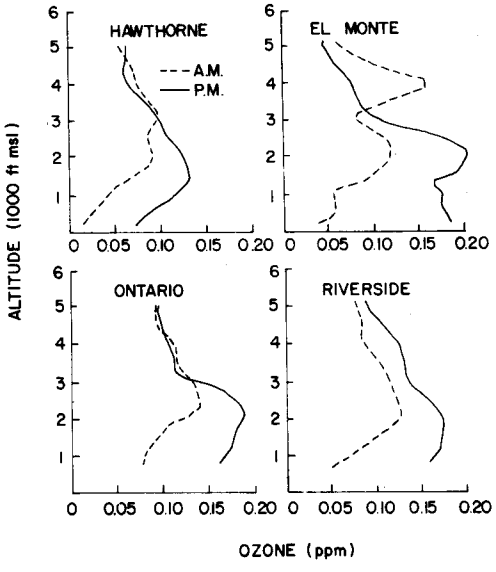

FIG. 6. Mean morning and afternoon O_3 profiles.

4. Aerosol parameters

a. Condensation nuclei count

Since small particles are much more numerous than large particles, the condensation nuclei count (CN) is primarily an index of the small-particle fraction of the aerosol. Particle size distribution measurements (Whitby *et al.*, 1972) have shown that particles under 0.1 μm in diameter account for nearly all of the CN. Particles in this size range are produced by combustion sources and (under conditions thought to be rare in ambient Los Angeles air) by homogeneous nucleation (Husar *et al.*, 1972; Whitby *et al.*, 1972). These particles coagulate rapidly with larger particles and with each other, so that the half-life of CN under typical Los Angeles smog conditions is on the order of an hour (Husar and Whitby, 1973; Husar *et al.*, 1972; Davies, 1974).

Mean profiles of CN are shown in Figs. 7 and 3d. Substantial CN gradients are observed near the surface in all four morning profiles and in the afternoon profile at Hawthorne. Above the mixing layer, CN counts drop to about 5×10^3 cm^{-3}, less than one-tenth of the counts within the mixing layer. Counts within the mixing layer are lowest at Riverside.

b. Light scattering coefficient

The light scattering coefficient (b_{scat}) of the atmosphere is determined largely by the concentration of particles with diameters in the range 0.1–1.0 μm (Ensor *et al.*, 1972), since these are the most efficient scatterers of visible radiation. Electron micrographs (Husar *et al.*, 1976) and chemical analyses (White, 1976) indicate that, under photochemical smog conditions, much of the aerosol in this size range is composed of secondary sulfates, nitrates and organics (Hidy *et al.*, 1974; Gartrell and Friedlander, 1975) produced from the gas phase. Some of this material is hygroscopic and b_{scat} is affected by high ambient relative humidities (Covert *et al.*, 1972). Once formed, the light scattering fraction of the aerosol is a fairly stable component of the atmosphere, with low surface loss rates (Chamberlain, 1967) and low coagulation rates (Husar *et al.*, 1972; Davies, 1974).

Of the four air quality parameters studied in this work, b_{scat} is the most stable and least sensitive to fresh emissions. These qualities are shown in the mean afternoon profiles of b_{scat} (Fig. 8). In all four profiles

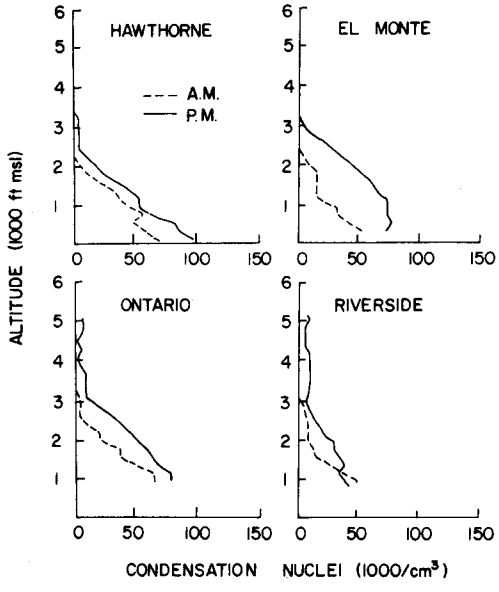

FIG. 7. Mean morning and afternoon condensation nuclei profiles.

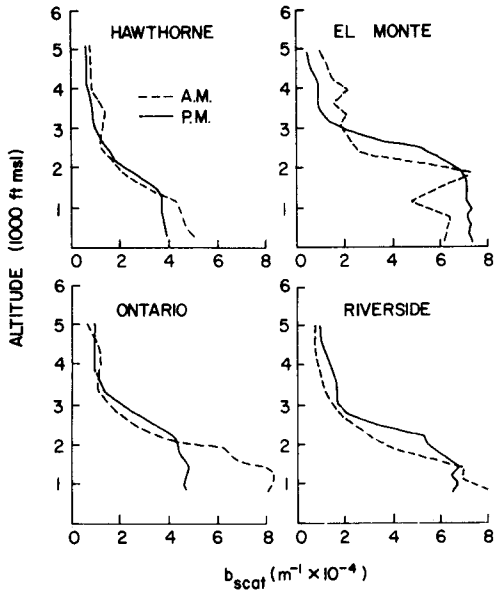

FIG. 8. Mean morning and afternoon b_{scat} profiles.

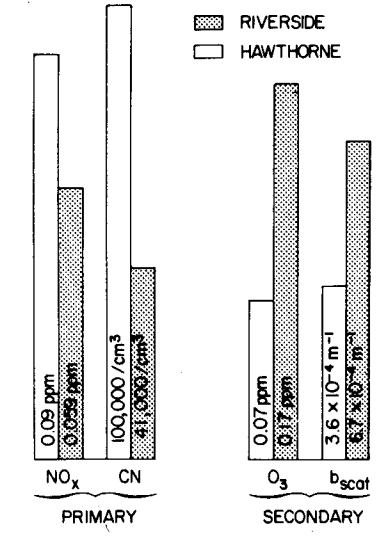

FIG. 9. Mean afternoon contaminant characteristics in first 200 ft above ground at Hawthorne and Riverside.

b_{scat} is fairly uniform through the mixing layer and drops to low levels above the mixing layer.

5. Pollutant aging

Fig. 1 shows that the characteristic air masses sampled over Hawthorne and Riverside in the afternoon have different histories. Hawthorne is only about 30 min of air parcel travel time downwind from the ocean. During those 30 min over land en route to Hawthorne, air passes over the San Diego Freeway and State Highway 1 and 107, as well as the heavily industrialized region around El Segundo. The afternoon soundings at Hawthorne thus sample predominantly fresh emissions, superimposed on the marine background (which itself may contain well aged anthropogenic contaminants).

Riverside, on the other hand, is from 3–6 h downwind of the ocean. As marine air moves inland, it first passes over the urban and industrialized areas of Los Angeles and Orange counties, then over the relatively rural region from the Chino Hills and Santa Ana mountains eastward to Riverside. As a result, most of the contaminants sampled in the afternoon soundings at Riverside have had 3–6 h to age en route.

The afternoon contaminant characteristics of the two locations are summarized and compared in Fig. 9 which shows the afternoon means for NO_x, O_3, CN and b_{scat} in the first 200 feet above ground level. It is apparent from Fig. 9 that the afternoon contaminant mixtures at Hawthorne and Riverside reflect the different histories of the air sampled, with significantly more NO_x and CN at Hawthorne and significantly more O_3 and b_{scat} at Riverside. Direct emissions account for most NO_x and CN, at which concentration can only decay in the atmosphere. High values of these parameters are thus generally indices of fresh emissions. Ozone, and a large fraction of the light scattering aerosol, are not emitted directly, but are produced in the atmosphere as secondary pollutants. High values of these parameters are generally indices of pollutant aging.

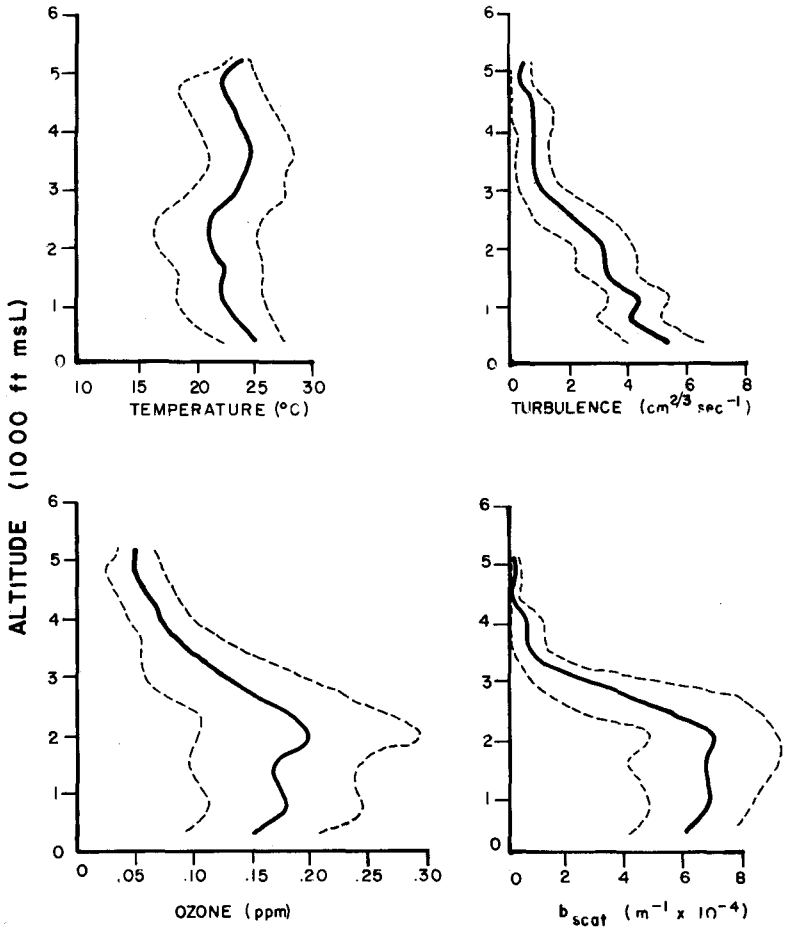

FIG. 10. The mean and standard deviation of temperature, turbulence, ozone and b_{scat} for the afternoon soundings at El Monte; solid line is the mean, dashed lines represent the mean ±1 standard deviation.

TABLE 2. Vertical integrals of the profiles and their standard deviations.

Meteorological parameters and pollutants		Hawthorne Mean	Hawthorne $\pm\sigma$	El Monte Mean	El Monte $\pm\sigma$	Ontario Mean	Ontario $\pm\sigma$	Riverside Mean	Riverside $\pm\sigma$
Temperature	A.M.	30180	4816	30850	2621	32310	4572	32310	4389
(°C-m)	P.M.	32740	4511	33470	5242	36700	3901	37060	4206
Turbulence	A.M.	2170	1622	1658	902	2682	1341	2219	951
($cm^{\frac{4}{3}}$ s^{-1}-m)	P.M.	2268	1402	3097	1256	3999	1609	3901	1244
Condensation nuclei	A.M.	19.51	10.5	15.12	7.5	34.62	15.9	20.48	9.0
(10^{12} m^{-2})	P.M.	31.70	13.9	36.58	14.9	53.16	22.4	36.09	20.2
Ozone*	A.M.	100	40	142	61	141	63	135	51
(ppm-m)	P.M.	140	69	185	79	199	86	210	77
NO_x	A.M.	76.8	38.0	79.2	51.0	132.9	35.0	108.5	46.0
(ppm-m)	P.M.	64.8	38.0	101.2	27.0	74.4	41.0	53.6	24.0
b_{scat}	A.M.	0.295	0.166	0.490	0.239	0.671	0.269	0.507	0.254
(dimensionless)	P.M.	0.254	0.135	0.541	0.219	0.349	0.202	0.476	0.312

* The units of the vertical integrals were obtained as ppm-meters (rather than ppm-ft).

6. Variability of the profiles

The profiles presented in the previous sections are averages over 24 days of sampling. In some instances, the variability about the mean is also of interest. For illustration purposes, the mean and the standard deviation of temperature, turbulence, ozone and b_{scat} for the afternoon soundings at El Monte are shown in Fig. 10. The standard deviations typically range from 15% of the mean to over 40% of the mean; the pollutant parameters vary more than temperature and turbulence.

Since it is not convenient to display the profiles with their standard deviations for all sites for each parameter for both morning and afternoon, we choose to represent each profile with a single number—its vertical integral. The integrations were carried out from ground level to 5200 ft MSL, and the results are listed in Table 2. The vertical integral of the light-scattering coefficient, i.e., the average optical depth of the summer smog layer, is between 0.25 at Hawthorne and 0.54 at El Monte. The integrals of condensation nuclei, ozone and NO_x do not have a simple physical meaning, but they may be useful in matching photochemical smog models with observed data. Also, the standard deviations of the integrals is a measure of the variability of the profiles themselves.

7. Summary and conclusions

Morning and afternoon "grand average" vertical profiles for Hawthorne, El Monte, Ontario and Riverside show an erosion of the nighttime radiation inversion during the day and increased temperatures and mixing due to surface heating in the inland areas. The semi-permanent subsidence inversion is also seen at higher level over the four sampling stations.

Average contaminant profiles indicate high values of primary pollutants (NO_x and condensation nuclei) in the source area near the coast at Hawthorne. On the other hand, the receptor site, Riverside (several hours of transport time inland), is characterized by high values of secondary pollutants, O_3 and b_{scat}, and low NO_x and CN. Morning profiles of O_3 at all locations indicate higher concentrations aloft than at the surface. This deficit is attributed to the scavenging of ozone by primary emissions.

Acknowledgments. This work was supported by the California Air Resources Branch. The authors appreciate the support and guidance provided by the late Dr. D. G. Hutchinson, Mr. Harris Samuels and Dr. Jack Suder.

REFERENCES

Blumenthal, D. L., T. B. Smith, W. H. White, S. L. Marsh, D. S. Ensor, R. B. Husar, R. B. McMurry, S. L. Heisler and P. Owens, 1974: Three-Dimensional Pollutant Gradient Study—1972–1973 program. Tech. Rep. MR174FR-1261, prepared for the California Air Resources Board by Meteorology Research, Inc. [NTIS PB 241982/66].

Chamberlain, A. C., 1967: Radioactive aerosols and vapours. *Contemp. Phys.*, **8**, 561–581.

Covert, D. S., R. J. Charlson and N. C. Ahlquist, 1972: A study of the relationship of chemical composition and humidity to light scattering by aerosols. *J. Appl. Meteor.*, **11**, 968–976.

Davies, C. N., 1974: Size distribution of atmospheric particles. *Aerosol Sci.*, **5**, 239–300.

Edinger, J. G., 1973: Vertical distribution of photochemical smog in the Los Angeles basin. *Environ. Sci. Tech.*, **7**, 247–252.

Ensor, D. S., R. J. Charlson, N. C. Ahlquist, K. T. Whitby, R. B. Husar and B. Y. H. Liu, 1972: Multiwavelength nephelometer measurements in Los Angeles smog aerosol. *J. Colloid Interface Sci.*, **39**, 242–251.

Gartrell, G., and S. K. Friedlander, 1975: Relating particulate pollution to sources: The 1972 California aerosol characterization study. *Atmos. Environ.*, **9**, 279–299.

Hidy, G. M., *et al.*, 1974: Characterization of aerosols in California. Final Report to California Air Resources Board under Contract 358. [NTIS: Vol. 2, PB248799/66; Vol. 4, PB247947/66].

Hill, A. C., 1971: Vegetation: A sink for atmospheric pollutants. *J. Air Pollut. Control Assoc.*, **21**, 341–346.

Husar, R. B., and K. T. Whitby, 1973: Growth mechanisms and size spectra of photochemical aerosols. *Environ. Sci. Tech.*, **7**, 241–247.

——, K. T. Whitby and B. Y. H. Liu, 1972: Physical mechanisms governing the dynamics of Los Angeles smog aerosol. *J. Colloid Interface Sci.*, **39**, 211–224.

——, W. H. White and D. L. Blumenthal, 1976: Direct evidence of heterogeneous aerosol formation in the Los Angeles smog. *Environ. Sci. Tech.*, **10**, 490–491.

Lundgren, D. A., 1970: Atmospheric aerosol composition and concentration as a function of particle size and of time. *J. Air Pollut. Control Assoc.*, **20**, 603–608.

MacCready, P. B. Jr., 1964: Standardization of gustiness values from aircraft. *J. Appl. Meteor.*, **3**, 439–449.

Whitby, K. T., R. B. Husar and B. Y. H. Liu, 1972: The aerosol size distribution of Los Angeles smog. *J. Colloid Interface Sci.*, **39**, 177–204.

White, W. H., 1976: Reduction of visibility by sulphates in photochemical smog. *Nature*, **264**, 735–736.